Selective Association between a Macrocyclic Nickel Complex and Extrahelical Guanine Residues†

Hui-Chen Shih,‡ Helina Kassahun,‡ Cynthia J. Burrows,§ and Steven E. Rokita*,‡

Department of Chemistry and Biochemistry, University of Maryland, College Park, Maryland 20742, and Department of Chemistry, University of Utah, Salt Lake City, Utah 84112

Received August 11, 1999

ABSTRACT: Nickel-dependent recognition and oxidation of guanine have been linked in part through the paramagnetic effects of nickel on the NMR of model oligonucleotide duplexes. Direct interaction between nickel and guanine N7 had originally been postulated from correlations between the efficiency of guanine oxidation and the environment surrounding its N7 position. ^{1}H and ^{31}P NMR spectra of DNA containing a single, isolated extrahelical guanine are consistent with selective binding of nickel to the N7 of this unique base over a background of nonspecific association to the phosphate backbone. The presence of a macrocyclic complex or simple salt of nickel did not detectably alter the structure of the duplex or extrahelical residue. Accordingly, nickel appeared to bind the extrahelical guanine N7 within the major groove as indicated by paramagnetic effects on the proton signals of nucleotides on the 5′ but not 3′ side of the nickel binding site. Similar ^{1}H NMR analysis of DNA containing a dynamic equilibrium of extrahelical guanine residues also suggested that the nickel complex did not affect the native distribution of structures. Oxidation of these sites by a nickel-mediated pathway consequently reflected their solvent accessibility in a general and metal-independent manner. The close proximity of the extrahelical guanines produced a composite of paramagnetic effects on each adjacent nucleotide resulting from both direct and proximal coordination of nickel.

Mapping the chemical and biochemical reactivity of DNA, RNA, and nucleic acid−protein assemblies is often used to characterize their complex three-dimensional structure (*1*−*4*). This approach is especially crucial for systems that remain intractable to higher resolution techniques based on crystallography or NMR spectroscopy. Although a single reagent may provide sufficient information on a specific issue of conformation, a broad range of reagents is more typically required for building a complete structural model. The diagnostic value of each reagent is directly related to its predictable activity. This in turn depends on the success of its past applications and an understanding of its mechanisms of recognition and reaction.

Our laboratories are currently exploring the utility of nickel- and cobalt-dependent probes of nucleic acid structure (*5*−*7*). These metals serve as the basis for a series of complementary reagents. Simple Co(II) salts promote conversion of monoperoxysulfate (HSO_5^-) to sulfate radical ($SO_4^{\cdot -}$), a reactive intermediate that exhibits an intrinsic selectivity for oxidizing accessible guanine bases (*8*). Macrocyclic complexes of nickel such as NiCR[1] appear to generate a related intermediate that remains metal-bound (*8*) and subject to additional selectivity dictated by the metal's specific affinity for guanine N7 (Scheme 1). When these sites

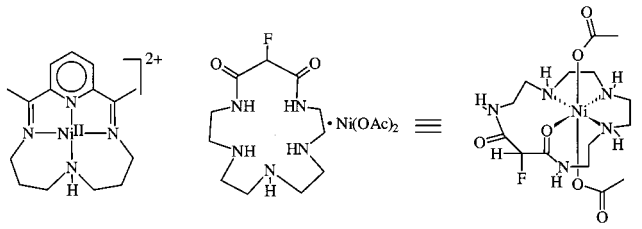

NiCR NiHFGN(OAc)$_2$ solid state structure

are inaccessible as in B-helical DNA, guanine oxidation is inefficient and varies with the ionization potential of each guanine residue (*9*). In contrast, guanine residues with accessible N7 positions are oxidized efficiently and quite specifically (*10*). This property has since been used in our laboratories to characterize extrahelical guanines in oligonucleotides (*11*) and regions of Z-DNA within plasmid DNA (*12*). Nickel complexes have additionally provided critical information on the structure and folding of many natural RNA sequences alternatively involved in catalysis, regulation, and structure (for example, see references *6* and *13*−*17*). A number of these examples have illustrated the superiority of the nickel reagents over their common alternatives, dimethyl sulfate and RNase T1.

The most active nickel reagents exist as 4-coordinate square planar complexes and exhibit little tendency to acquire axial ligands in their initial +II oxidation state (*18*). Selective association with DNA is established only after axial ligation is induced by oxidizing the nickel to its +III state which in

† This research was supported by the National Institutes of Health (GM-47531).

* To whom correspondence should be addressed. (Phone 301-405-1816, fax 301-405-9375, e-mail sr101@umail.umd.edu).

‡ University of Maryland.

§ University of Utah.

[1] Abbreviations: NiCR, (2,12-dimethyl-3,7,11,17-tetraazabicyclo-[11.3.1]heptadeca-1(17),2,11,13,15-pentaenato)nickel(II) perchlorate; NiHFGN, (15-fluoro-1,4,7,10,13-pentaazacyclohexadecan-14,16-dione)-nickel(II).

10.1021/bi991877h CCC: $18.00
Published on Web 10/23/1999

Scheme 1: Proposed Mechanism for Selective Oxidation of Guanine

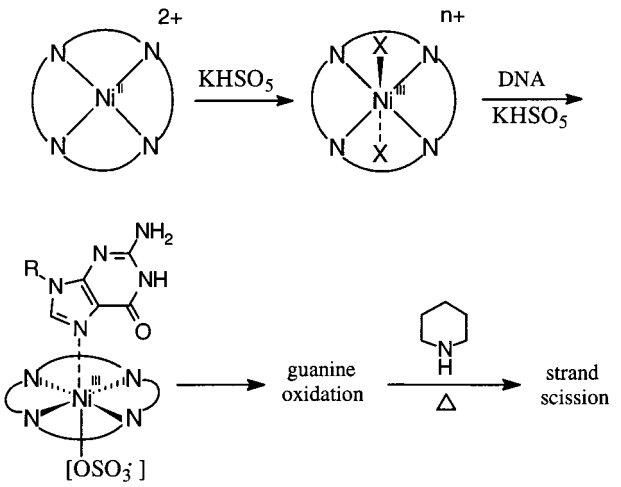

turn adopts octahedral, 6-coordinate geometry (*11, 18*). Guanine N7 is the preferred site for nucleobase coordination by nickel (*19*), but the phosphate backbone of DNA also exhibits some affinity to this metal as well (*20*). The crystal structure of GMP and nickel illustrates inner-sphere coordination to guanine N7 and outer-sphere coordination to the phosphate group via nickel-bound water (*21*). Although crystallography (*22*) and NMR (*23*) have also detected interactions between nickel and guanine N7 within duplex DNA, association is limited by the steric environment of the B-helical major groove (*22*−*25*). Perturbations in the groove structure can enhance nickel binding (*22*), and, similarly, nickel binding can often induce conformational changes in duplex DNA to enhance access of guanine N7. For example, both simple nickel salts (*26*) and certain nickel complexes (*11*) promote conversion of poly(dG-dC) from its B- to Z-helical form through coordination to guanine N7.

The constraints of binding nickel to guanine N7 are consequently expected to control the selectivity of the nickel complexes used as structural probes. Profiles of guanine modification have repeatedly suggested such a correlation (*5, 6, 10, 12*), but a direct link between binding and reactivity is described for the first time in this article. A nickel complex that mimics the reactive and transient coordination illustrated in Scheme 1 was recently shown by the paramagnetic effects of nickel on the nucleotides' ^{1}H NMR spectra to bind the N7 of 5′-GMP > 5′-IMP > 5′-AMP (*11*). A more stable derivative of this complex, NiHFGN, which also exhibits octahedral coordination and an equal affinity for guanine N7 (*11, 27*), has now been used in an analogous approach to compare reaction and recognition of extrahelical guanines within duplex oligonucleotides. While the complexity of paramagnetic effects precludes detailed model building, the effects clearly localize around the reactive guanine residues.

MATERIALS AND METHODS

Materials. The macrocyclic metal complexes NiCR$(ClO_4)_2$ (*28*) and NiHFGN$(OAc)_2$ (*29*) were synthesized by Drs. James G. Muller and Chien-Chung Cheng, respectively. $NiCl_2$, NaCl, NaH_2PO_4, Na_2HPO_4, and $KHSO_5$ (Oxone) were used as received. All aqueous solutions were prepared with purified water (Nanopure, Sybron/Barnsted). 5′-DMT-oligonucleotides were purchased from Keystone Lab in a 15 μmol scale and purified with a self-packed POROS 20R2 reverse phase column (PerSeptive Biosystems, Framingham, MA) using a linear gradient (5 min) of 0−30% acetonitrile in 0.1 M triethylammonium acetate, pH 7.0 (5 mL/min). Samples were detritylated with 80% aqueous acetic acid for 5 min at room temperature, extracted with ethyl acetate, and finally lyophilized to dryness. The purified oligonucleotides were extensively dialyzed against 10 mM sodium phosphate (pH 7.0) and 2 mM EDTA, 10 mM phosphate buffer (pH 7.0) alone, and finally water. The samples were then lyophilized to dryness and stored at −20 °C. 5′-^{32}P-Radiolabeled oligonucleotides were prepared from [γ-^{32}P]ATP and T4 polynucleotide kinase under standard conditions.

DNA Oxidation. Oligonucleotides cg4 and g3 (50 μM, 2 nCi) were individually combined with NaCl (100 mM), NiCR (50 μM), sodium phosphate (10 mM, pH 7.0), and the appropriate oligonucleotides in excess (250 μM) to form duplex DNA containing extrahelical guanines. Reaction was initiated by addition of 0.5 mM $KHSO_5$ and maintained under ambient conditions for 30 min. Samples (10 μL) were quenched with β-mercaptoethanol (20 μL), precipitated with ethanol, resuspended in piperidine (0.2 M, 20 μL), and heated to 90 °C for 30 min (*30*). DNA fragmentation was analyzed by gel electrophoresis (20% polyacrylamide, 8 M urea) and autoradiography. The relative reactivity of competing sites was quantified by densitometry (Enprotech Integrated Separation Systems) and calculated as the fraction of total products.

NMR Sample Preparation. Equimolar concentrations of the appropriate oligonucleotides (2 mM for 2-D ^{1}H NMR, 0.5 mM for 1-D ^{1}H NMR) were combined with sodium phosphate (10 mM) in 500 μL of D_2O (99.9% D, pD 7.0) for studying nonexchangeable protons or 80% H_2O/D_2O (pH 7.0) for studying exchangeable protons. Samples were annealed by heating to 90 °C for 3 min and then slow-cooling to room temperature (>3 h). Oligonucleotide concentrations were calculated from their A_{260} values and extinction coefficients estimated from the sum of nucleotide absorptivity as affected by adjacent bases (*31*).

NMR Measurements. ^{1}H NMR data were acquired on Bruker AMX-600 (SUNY, Stony Brook) and AMX-500 (University of Maryland, College Park) NMR spectrometers. Sodium 3-(trimethylsilyl)propionate-*2,2,3,3-d*$_4$ was added as an internal standard for all ^{1}H measurements. For samples in D_2O, the HOD signal was suppressed with low-power presaturation irradiation, and the remaining proton signals were recorded with a spectral width of 11 ppm and 16K data points (25 °C). For samples in 80% H_2O/D_2O, a 1-1 echo pulse sequence was used to suppress the solvent signal, and the remaining proton signals were recorded with a spectral width of 20 ppm and 32K data points (4 °C). These latter analyses were performed at low temperature in order to detect the imino protons of extrahelical guanines (*32*).

DQF−COSY spectra were acquired from D_2O solutions in the pure-absorption mode with quadrature detection using time-proportional phase incrementation. A total of 512 t_1 increments with 4096 data points in t_2 were collected for each experiment with a spectral width of 11 ppm and a delay of 1.3 or 1.5 s. Phase-sensitive NOESY spectra were acquired from D_2O solutions with quadrature detection using time-proportional phase incrementation. A total of 512 t_1 increments with 2048 data points in t_2 were collected for each

experiment with a spectral width of 11 ppm, a delay of 1.3 or 1.5 s, and a mixing time of 250 ms.

^{31}P NMR (200 MHz) spectra were acquired from D_2O solutions at 25 °C with a spectral width of 20 ppm and 64K data points. Phosphate buffer (pD 7.0) was used as an internal standard. All NMR data were zero-filled once and multiplied by a sine-bell window function prior to Fourier transformation using *Felix* software (version 2.3).

Titration with NiHFGN and $NiCl_2$. NMR spectra were acquired after addition of each aliquot (1−3 μL) of a concentrated nickel stock solution (5 mM). The effects of the paramagnetic metal on chemical shifts are illustrated by plotting chemical shift (δ) in ppm vs the molar ratio of nickel to duplex DNA. EDTA (0.7 mM) was added to the solution of g3/cg4 prior to titration with $NiCl_2$, and, consequently, the molar ratio of nickel is presented as the excess over EDTA. Only this sample required such treatment to minimize spectral perturbations from contaminating metals.

T_m Determinations. Oligonucleotides (3 μM each) in 100 mM NaCl and 10 mM sodium phosphate, pH 7, were annealed by heating to 90 °C for 5 min and then slow cooling to room temperature over approximately 3 h. The appropriate concentration of NiHFGN or $NiCl_2$ was added after the annealing process. Thermal denaturation of DNA was monitored by the increase in absorbance at 260 nm using an HP 8452A spectrophotometer and Peltier temperature controller (5 °C intervals from 10 to 75 °C). Data were fit to a two-state transition (manufacturer's software), and its derivative was used to determine the melting temperatures (T_m).

RESULTS

Duplex DNA Containing a Unique Extrahelical Guanine. The DNA sequences first chosen for directly relating the reaction and recognition specificity of nickel were derived from a model duplex that had already been extensively characterized by NMR and energy minimization (*32*, *33*). This system contained a single extrahelical guanine that had been shown to stack into the duplex and yet maintain some solvent exposure by bending the helix axis (*33*). For our studies, A-T base pairs were appended to both termini of the original sequences in order to avoid competition between extrahelical and terminal guanines (Figure 1). Proton resonances were assigned sequentially from NOESY and COSY spectra following standard procedures (*34*−*36*) (Supporting Information) and were consistent with the parent sequences (*37*).

Selective Oxidation of the Extrahelical Guanine. The target selectivity of NiCR was originally identified through a series of oligonucleotide studies (*30*) which would predict a unique reactivity of G17, the extrahelical guanine in g3/cg4. This site was indeed the only target of NiCR and $KHSO_5$. Selective oxidation was detected after subsequent strand fragmentation induced by hot piperidine (Figure 1, lane 2). No reaction occurred in the absence of NiCR (lane 1), and no spontaneous fragmentation was detected in the absence of piperidine treatment (lane 3). According to the mechanism outlined in Scheme 1, the specificity of oxidation should be equivalent to the specificity of nickel binding. However, the octahedral Ni(III) intermediate generated by NiCR was too transient for physical characterization. An alternative complex was consequently chosen for study of nickel−DNA interactions. This complex, NiHFGN, in its stable +II oxidation state was already known to form an octahedral complex with exchangeable acetate ions at both axial positions and share many of the expected binding properties of NiCR in its reactive +III oxidation state (*11*, *27*).

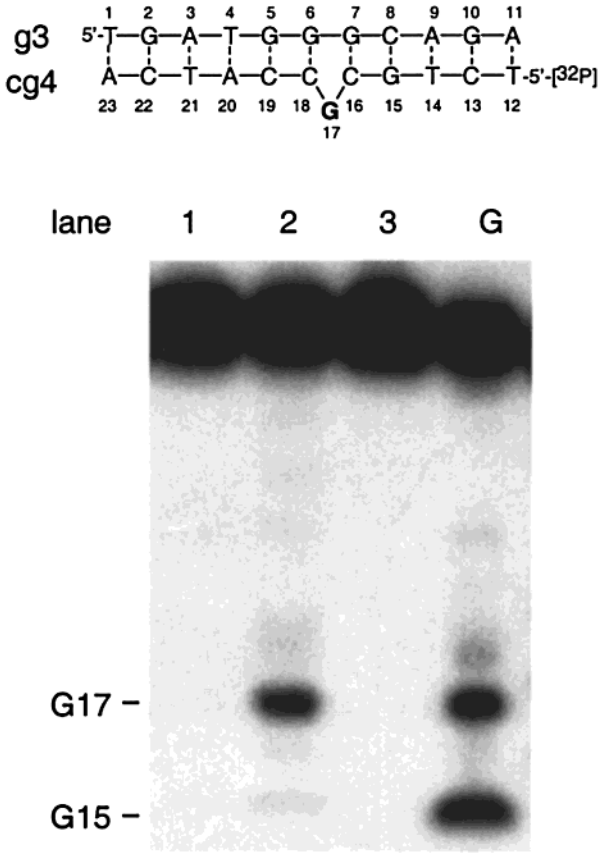

FIGURE 1: NiCR-dependent modification of g3/cg4. The duplex formed by g3 and 5′-^{32}P-labeled cg4 was treated with $KHSO_5$ in the absence (lane 1) and presence of NiCR (lanes 2 and 3). Samples of lanes 1 and 2 were subsequently heated in the presence of piperidine whereas the sample of lane 3 was analyzed directly. A guanine marker lane was produced by standard dimethyl sulfate reaction of 5′-^{32}P-labeled cg4 (lane G) (*48*). See Materials and-Methods for experimental details.

Paramagnetic Effect of NiHFGN on ^{1}H NMR of g3/cg4. A general broadening of all proton signals of g3/cg4 was evident as NiHFGN approached a concentration equimolar to the duplex. This result suggested the presence of a background, nonspecific interaction between the paramagnetic complex and DNA. A subset of proton signals also exhibited additional sensitivity to NiHFGN that is consistent with a unique and specific recognition of G17. Both the general and selective modes of association appeared in fast exchange since no new proton signals were detected upon addition of NiHFGN.

The aromatic region of the proton spectra that includes signals for guanine H8 and cytosine H6 was most indicative of the specific association with NiHFGN (Figure 2A). Both protons reside in the major groove, and guanine H8 is directly adjacent to the proposed site of ligation, guanine N7. The H8 of G17 displayed the greatest change in chemical shift and relaxation (Figure 2B). In contrast, the H8 protons of G2 and G10 were affected by NiHFGN at only background levels. Guanine residues (G5, G6, and G15) toward the 5′-

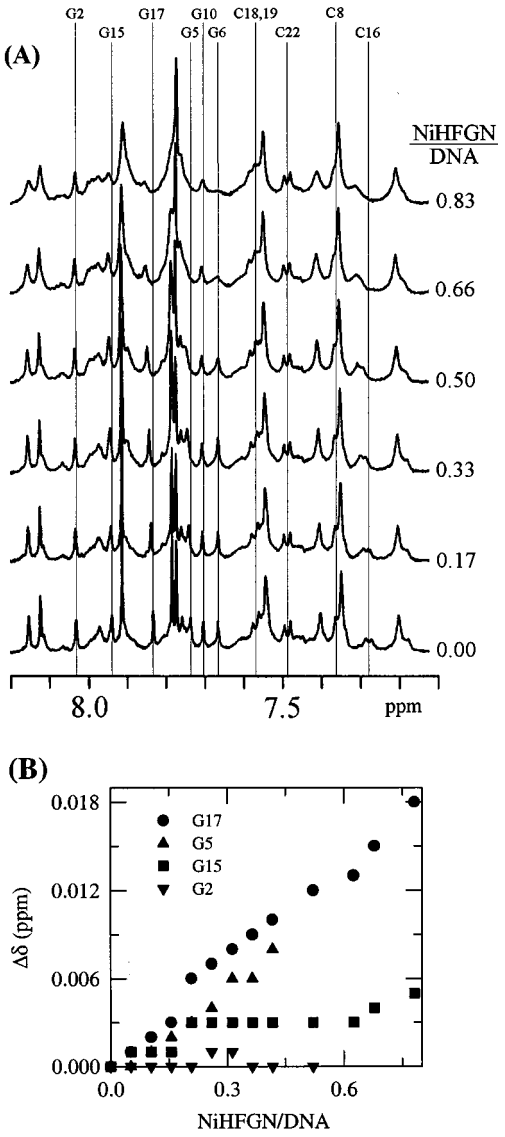

FIGURE 2: (A) ^{1}H NMR (500 MHz) spectra of duplex g3:cg4 containing an extrahelical guanine in the presence of varying concentrations of NiHFGN (25 °C). Notable guanine H8 and cytosine H6 protons are identified by their nucleotide position. The molar ratios of metal to oligonucleotide duplex are indicated on the right. (B) Shifting of selected guanine H8 signals was determined as a function of the molar ratio of metal to DNA. $\Delta\delta$ (ppm) were determined from the ^{1}H NMR spectra illustrated in part A and from intervening titration points.

side of the extrahelical guanine on both strands expressed an intermediate sensitivity to NiHFGN. In this case, perturbation of the H8 signals of G5 and G15 was manifested by line broadening and shifting, whereas only line broadening was apparent for the H8 signal of G6. The H8 signal of G7 (7.90 ppm) was unusually broad in the absence of NiHFGN and not easily detected under these and previous experimental conditions due to its uniquely long correlation time (*33*). This property has been attributed to the structural perturbations caused by the extrahelical base G17. Such effects are not shared by the neighboring residue G6 (*33*). Cytosine C16, the direct 5′-neighbor of G17, was the only cytosine specifically perturbed by NiHFGN as evident from the shifting and broadening of its H6 signal. Even C18, the 3′-neighbor of G17, remained relatively unaffected by the paramagnetic complex.

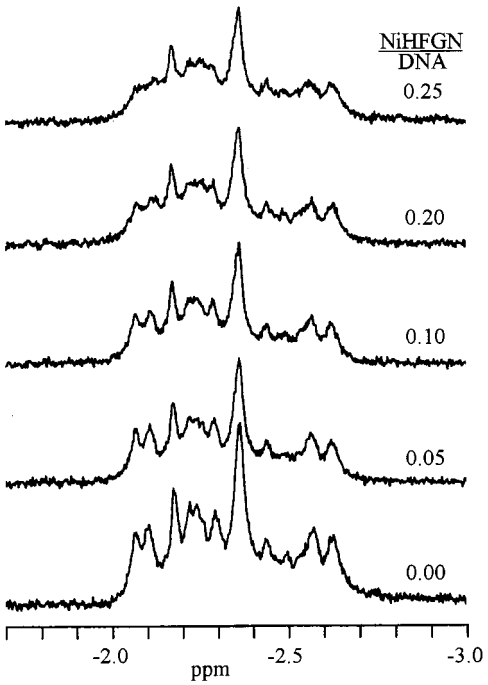

FIGURE 3: ^{31}P NMR (200 MHz) spectra of duplex g3:cg4 containing an extrahelical guanine in the presence of varying concentrations of NiHFGN (25 °C). The molar ratios of metal to duplex are indicated on the right.

The imino protons of g3/cg4 were also monitored during titration with NiHFGN under comparable conditions to the studies above (Supporting Information). As noted from previous NMR characterization, the imino proton of the extrahelical G17 is far upfield relative to its counterparts involved in Watson−Crick hydrogen bonding (*32*). Disruption or mere perturbation of base pairing can affect the imino protons' chemical shift and signal shape greatly (*32*, *36*), and similar, but independent, effects could additionally be induced by proximal binding of a paramagnetic ion. In the presence of increasing concentrations of NiHFGN, all of the imino proton signals progressively broadened, and no localized effects were observed. Titration was discontinued after addition of 0.35 mol equiv of NiHFGN since the weak signal of G17 became undetectably broad. Under these conditions, no changes in the chemical shift of this or other signals were apparent. Thus, base pairing within this duplex was not disturbed significantly. Similarly, NiHFGN did not strongly displace or bind adjacent to the imino proton of G17 within the duplex interior, and no internal proton transfer from G N1 to C N3 was evident, in contrast to previous suggestions based on UV spectral titrations of DNA with Ni^{2+} (*38*).

Paramagnetic Effect of NiHFGN on ^{31}P NMR of g3/cg4. Complexation between NiHFGN and the phosphate backbone of g3/cg4 was characterized by ^{31}P NMR in the presence of increasing concentrations of the metal complex (Figure 3). Significant nonspecific association was anticipated from the general affinity of the anionic backbone for cations. This was indeed observed through a general relaxation of all ^{31}P signals in the presence of the paramagnetic nickel. A unique binding site for nickel might also have been established by the N7 of G17 and an adjacent phosphate. This type of coordination has been previously observed in cocrystals formed by simple nickel salts and either 5′-GMP (*21*) or an oligonucleotide duplex (*22*). Within the limitations of the

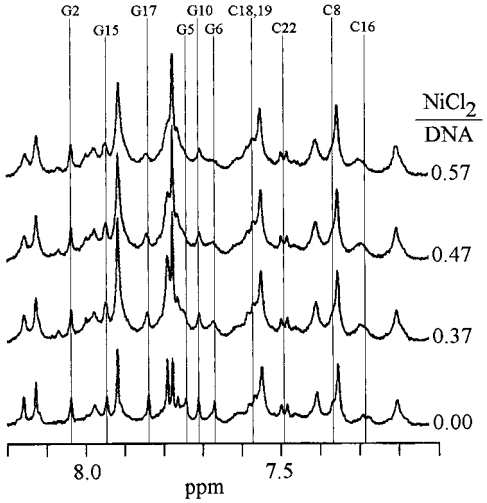

FIGURE 4: ^{1}H NMR (500 MHz) spectra of duplex g3:cg4 containing an extrahelical guanine in the presence of varying concentrations of $NiCl_2$ (25 °C). Notable guanine H8 and cytosine H6 protons are identified by their nucleotide position. The molar ratios of metal to duplex are indicated on the right.

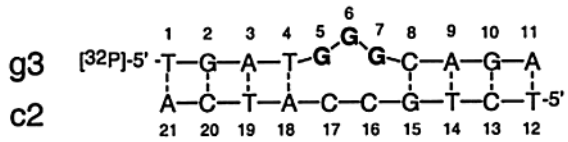

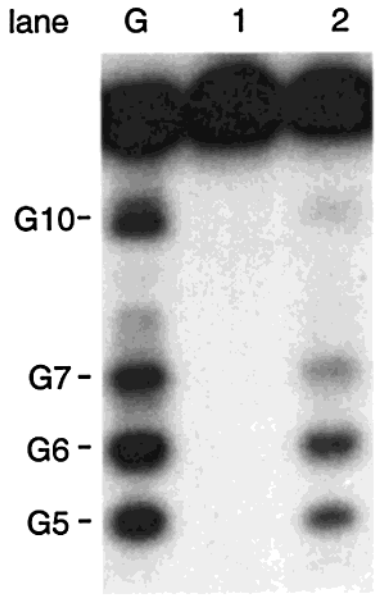

FIGURE 5: NiCR-dependent modification of g3:c2. A guanine marker lane was produced by standard dimethyl sulfate reaction of 5′-[^{32}P]-labeled g3 (lane G) (*48*). The duplex formed by c2 and 5′-[^{32}P]-labeled g3 was treated with NiCR and $KHSO_5$ (lane 1) and subsequently heated in the presence of piperidine (lane 2). See Methods for experimental details.

spectral resolution illustrated in Figure 3, no individual ^{31}P signal expressed a dramatic change in chemical shift or relaxation that would suggest selective binding.

Paramagnetic Effect of $NiCl_2$ on ^{1}H NMR of g3/cg4. Titration experiments were repeated using $NiCl_2$ to evaluate the steric limitations of coordination to g3/cg4 (Figure 5). If the macrocyclic ligand of NiHFGN restricted its recognition of noncanonical structures within duplex DNA, then a simple nickel salt might have demonstrated a greater proficiency for association to such structures. This in turn would have led to a greater occupancy at the G17 site and hence more significant perturbation of the NMR signals associated with this region. $NiCl_2$ was indeed more effiicent than NiHFGN at broadening the H8 signals of G5, G6, and G17 and the H6 signal of C16. However, no changes in chemical shift were detected for any guanine signals including the extrahelical residue G17. Only the H6 of C16 exhibited any detectable shift in its signal. The general relaxation of the remaining protons was likely caused by nonspecific interactions between DNA and nickel.

Thermal Stability of Duplex DNA in the Presence of $NiCl_2$ and NiHFGN. B-Helical DNA is typically stabilized by metal ions such as Mg^{2+} that coordinate to the phosphate backbone. In contrast, metal ions such as Cu^{2+} destabilize DNA by coordinating to the nucleobases (*20*). Simple metal salts of Co(II), Ni(II), and Mn(II) were previously found to act in an intermediate manner by binding to both phosphate groups and nucleobases of calf thymus DNA (*20*). This behavior had formally been examined qualitatively by determining the thermal denaturation of DNA (T_m) in the presence of varying concentrations of metals. This analysis has now been repeated for the specific oligonucleotide system described here. First, the effect of $NiCl_2$ was determined for the parent duplex formed by g3 and its complement d(TCTGCCCATCA) (c3). The T_m value for this canonical structure remained within 1% of 51 °C in the presence or absence of a 67-fold molar excess of $NiCl_2$ (200 μM). Insertion of the extrahelical guanine to form g3/cg4 depressed the T_m value to 37 °C, but no further change was observed upon addition of $NiCl_2$ (200 μM). NiHFGN (0−200 μM) also did not detectably affect the T_m of g3/cg4. Interestingly, the canonical duplex g3/c3 was slightly destabilized by 200 μM NiHFGN as indicated by a 4 °C decrease in its T_m (47 °C). Still, the overall effect of nickel on DNA stability was minimal. Whatever destabilization existed from nucleobase interactions favored in single-stranded DNA was generally balanced by stabilization from phosphate interactions favored in duplex DNA. A less likely alternative explanation would require that neither interaction exists at temperatures approaching the transition betweeen single- and double-stranded DNA.

DNA Containing an Extrahelical Guanine within a G-Tract. Correlation between recognition and reaction of the nickel complexes was extended to the duplex g3/c2, which establishes an equilibrium of conformations with three alternative extrahelical residues, G5, G6, or G7 (Scheme 2). Similar to g3/cg4, this system also derives from a set of parent sequences that were previously subjected to extensive structural and thermodynamic characterization by NMR (*32*). The fractional population of each species could now be used to anticipate the relative reactivity of each extrahelical guanine with NiCR and the extent to which each would be affected by the paramagnetic complex NiHFGN. In addition, the influence of nickel on the equilibrium of structures could be determined directly for the first time as well.

Competitive Oxidation of Extrahelical Guanines in a Dynamic Equilibrium. NiCR again promoted oxidation with the predicted specificity. The fully paired guanine (G10) of g3/c2 maintained very low reactivity, whereas the residues (G5, G6, and G7) that rapidly interconvert between their paired and extrahelical forms were much more reactive

Scheme 2: Equilibrium of Structures Formed by g3/c2

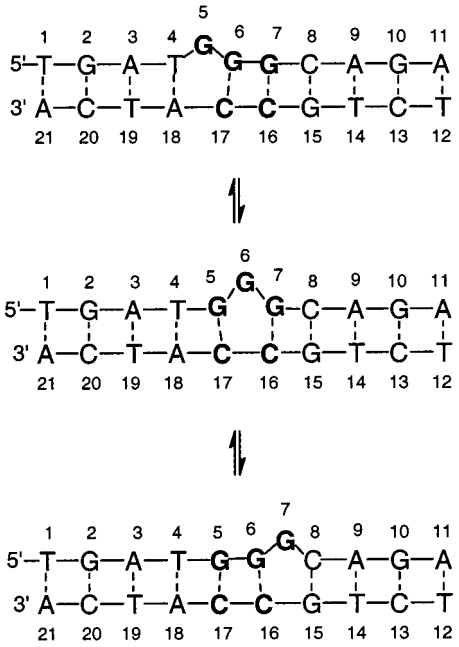

(Figure 5, lane 2). Oxidation efficiency was not uniform for these guanines and instead reflected their individual propensity for adopting an extrahelical conformation (*32*). As expected, no spontaneous strand fragmentation was detected after incubation with NiCR and $KHSO_5$ (lane 1). Consequently, all of the reaction likely proceeded through direct coordination between the transient octahedral nickel intermediate and the extrahelical target base (Scheme 1).

Paramagnetic Effect of NiHFGN on ^{1}H NMR of g3/c2. The equilibrium of structures formed by g3/c2 exhibited a similar response to the paramagnetic complex NiHFGN as that illustrated previously for g3/cg4 (Figure 2). Substoichiometric concentrations of NiHFGN were sufficient to induce a general background relaxation of all ^{1}H signals of g3/c2. Again, the aromatic region of the NMR spectrum was most diagnostic of the selective effects of NiHFGN above this general background (Figure 6A). G2 and G10 are distal to the potential sites of nickel coordination, and consequently their H8 proton signals were only affected at background levels. Even the H6 protons of C16 and C17 that form the two C-G base pairs adjacent to the extrahelical G (Scheme 2) were only slightly more sensitive than background to NiHFGN. However, the 5′-neighbor of the extrahelical G sites, G15, did show modest sensitivity to the paramagnetic complex through a chemical shift and an enhanced relaxation of its H8 proton signal (Figure 6B). The chemical shifts of two out of the three potential extrahelical guanines (G5 and G6) were most affected by NiHFGN, and all three (G5, G6, and G7) were selectively broadened in the presence of NiHFGN. Finally, the imino signals of g3/g2 were equivalent to those of the previous model system (*32*) and were not subject to any specific or localized perturbation caused by NiHFGN. These experiments were limited to a NiHFGN concentration of 25 mol % since greater concentrations rendered the signals too broad to observe.

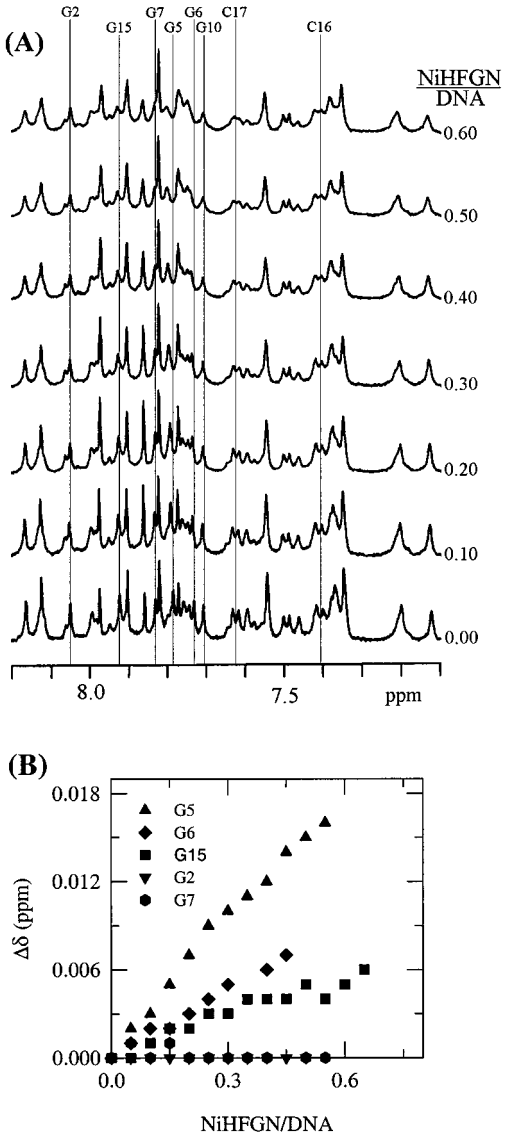

FIGURE 6: (A) ^{1}H NMR (500 MHz) spectra of duplex g3:c2 containing an extrahelical guanine in the presence of varying concentrations of NiHFGN (25 °C). Notable guanine H8 and cytosine H6 protons are identified by their nucleotide position. The molar ratios of metal to duplex are indicated on the right. (B) Shifting of selected guanine H8 signals was determined as a function of the molar ratio of metal to DNA. $\Delta\delta$ (ppm) were determined from the ^{1}H NMR spectra illustrated in part A and from intervening titration points.

DISCUSSION

Association between nickel and guanine N7 was initially proposed to explain the selectivity of structural probes based on nickel since their activity correlated to the nature of this common site of ligation (*5*, *6*). Binding at guanine N7 had been shown repeatedly by a number of laboratories to dominate interactions between nucleobases and nickel (*19*) although nonspecific association with the phosphate backbone had also been identified with polynucleotides (*20*). Direct coordination of nickel rather than mere exposure to a diffusible oxidant is thought to control specificity (Scheme 1) since reaction is influenced by the electrostatic as well as steric environment surrounding guanine N7 (*10*). This site typically resides on the major groove surface of duplex DNA, and consequently interaction with N7 is limited by the steric presence of its 5′-neighboring residues (*22*−*25*). Variation in the nucleophilicity, and hence ligand strength, of GN7 appears to control the sequence selectivity of nickel binding to canonical duplex DNA (*23*). However, helical residues

are not significant targets of the nickel reagents. Extrahelical guanine residues are most efficiently oxidized by nickel and thus should represent the principal site of nucleobase coordination.

Correlation between reaction and binding selectivity was expedited by investigating a series of oligonucleotide structures containing extrahelical guanines that had already been characterized by NMR in the absence of nickel (*32, 33*). Extensive information on both the conformation and stability of each structure was available, and one representative set of sequences had already expressed a reactivity with NiCR that was consistent with the equilibrium of structures identified by NMR (*11*). Prior investigations had similarly suggested that NiHFGN would be an appropriate model for the reactive nickel intermediate responsible for selective oxidation of guanine since this macrocyclic complex has an octahedral geometry and binds to the N7 of GMP with release of acetate (*11, 27*). The paramagnetic properties of this complex have now provided sufficient NMR data for a qualitative description of its interaction with DNA.

The presence of NiHFGN introduced a general background of line broadening for all signals in the ^{1}H and ^{31}P NMR spectra of the oligonucleotides as a result of weak and nonspecific association. More interestingly, the aromatic region of the ^{1}H spectra illustrated a subset of signals that were also selectively broadened and shifted due to specific and localized binding of nickel. All interactions between nickel and DNA were in fast exchange as expected from previous results on simple metal salts of Mn^{2+}, Co^{2+}, Ni^{2+}, and Zn^{2+} (*23, 39*). In contrast, palladium (*40*) and platinum (*41*) complexes often bind to DNA in slow exchange.

Duplex DNA Containing a Single, Isolated Extrahelical Guanine. The extrahelical G17 of g3/cg4 was the sole target of oxidation by NiCR (Figure 1), and the N7 of this residue was also the predominant site of NiHFGN binding as determined by ^{1}H NMR (Figure 2). The proton G17 H8 immediately adjacent to the N7 position exhibited the most prominent sensitivity to NiHFGN. Substoichiometric concentrations of this metal complex caused significant line broadening and maximum shifting of the resonance of G17 H8. For octrahedral complexes of Ni(II), line broadening has been attributed to dipolar coupling, an anisotropic through-space effect. In contrast, line shifting has been attributed to hyperfine coupling through Fermi contact, a direct and isotropic effect (*42*−*46*). Consequently, line shifting is most indicative of an intimate association with the paramagnetic metal and its ligands. Line broadening may be used in these experiments only to suggest general proximity. Greatest contact between NiHFGN and g3/cg4 thus occurs at G17, the extrahelical residue.

Earlier studies indicated that G17 remained stacked in the duplex by means of a small local bend in the helix axis (*33*). If nickel coordination did not disrupt this structure, then binding to guanine N7 would remain within the confines of the expanded major groove. This in turn would predict that nucleotides on both strands in the 5′ direction of G17 would also be susceptible to the paramagnetic effects of nickel (*22*−*25*). Indeed, the second and third most shifted H8 signals were those of G5 and G15 (Figure 2B). Similarly, the signal for H6 of C16 but not H6 of C18 was shifted in the presence of NiHFGN. Although the G6 signal was subject to extensive line broadening, no shifting was evident (Figure 2A). This residue is therefore likely to be in close proximity to, but not in contact with, NiHFGN. Since G7 is on the 3′ side of the extrahelical residue, minimal perturbation would have been expected. This could not be tested due to its very broad H8 signal prior to titration with nickel. Guanine residues such as G2 that are far from the extrahelical G17 showed only background levels of perturbation in the presence of NiHFGN. This first oligonucleotide duplex illustrates that the influence of NiHFGN was not detected uniformly within the major groove but rather limited to the vicinty of G17.

The overall effect of NiHFGN on the extrahelical guanine is substantially reduced when compared to its equivalent effect on GMP (*11*). As little as 10 mol % NiHFGN significantly perturbed the H8 signal of GMP, and the presence of stoichiometric nickel would have broadened the signal to the extent that it would not be observed under standard conditions. For example, the acetate ligands of NiHFGN were not detectable until displaced from nickel by addition of DNA. In contrast to even an extrahelical guanine within duplex DNA, GMP offers unencumbered access to its N7 position and the ability to form a macrochelate with the attached phosphate group (*21*). Binding at guanine N7 not only is more constrained within a DNA helix but also is in competition with a continuum of nonspecific binding along the phosphate backbone. Neither mode appears to dominate since the thermal stability of g3/cg4 was not enhanced or decreased by NiHFGN association with the backbone or guanine, respectively. The NMR and thermal measurements can both be explained by a low occupancy of NiHFGN at its unique coordination site of G17. This does not preclude the basis for recognition and reaction by NiCR since oxidation is thought also to originate from only a low steady-state concentration of a nickel−DNA complex (Scheme 1) (*11*). Even solid-state structures of DNA containing cobalt, copper, and nickel do not exhibit full occupancy at guanine N7 (*22, 24, 47*).

$NiCl_2$ forms an octahedral hydrate in aqueous solution and had much the same effect as NiHFGN on the ^{1}H NMR of g3/cg4. Again, general and specific association with the DNA was evident. All proton signals exhibited at least a low level of broadening by the paramagnetic ion. Protons in the major groove surrounding G17 N7 were most strongly affected (Figure 4). Perturbation in this case was only observed through dipolar line broadening of the proton signals. No shifting was apparent, and this is consistent with the very small hyperfine coupling constant of the Ni(II) hydrate (*45*). The magnitude of the dipolar effect caused by the simple nickel salt was suppressed to a greater extent than that of NiHFGN when comparing titrations of GMP (*11*) and g3/cg4. This may be explained by an even lower occupancy of the hydrated ion at the G17 site due to an enhanced affinity for the phosphate backbone. Such a change would have to be modest since $NiCl_2$ did not increase the thermal stability of g3/cg4. Still, the simple salt expressed a lower affinity than NiHFGN for guanine N7 when used to promote a B- to Z-helical transition through coordination of this site (*11*).

Duplex DNA Containing an Equilibrium of Alternative Extrahelical Guanine Residues. The use of nickel(II) reagents such as NiCR has proven to be a simple yet accurate method for measuring the equilibrium population of competitive structures. This activity is substantially more subtle than merely detecting extrahelical or highly exposed guanine

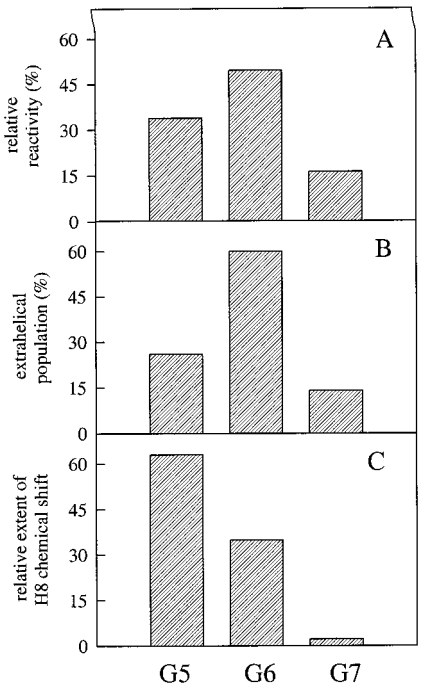

FIGURE 7: (A) Relative reactivity of each potentially extrahelical guanine of g3:c2 in comparison to the sum of reaction at these residues. (B) Relative abundance of each extrahelical structure in the presence of 25 mol % NiHFGN as determined by the imino proton chemical shifts (*32*). (C) Relative sensitivity of extrahelical guanines to the presence of NiHFGN as detected by the change in guanine H8 chemical shift. The $\Delta(\delta)$/[NiHFGN] for each residue was calculated by linear least-squares analysis of the data in Figure 6B and compared to the sum of these slopes.

residues since target recognition cannot itself affect the distribution of conformers. The resting states of the active nickel reagents are square planar and demonstrate little affinity for additional ligands provided by nucleobases (*11*, *18*). Binding is only expected to occur between the transient nickel(III) octahedral intermediate and the N7 of accessible guanine residues (Scheme 1). Consequently, this association should be driven by the native conformations of DNA rather than by independent variables introduced by the nickel. Preliminary analysis of an extrahelical guanine within a track of five guanines (*11*) and related investigations described here using a track of three guanines (g3/c2, Figures 5 and 7A) illustrate the remarkable similarity between the profile of guanine oxidation by NiCR and the corresponding DNA conformations defined by past NMR study (*32*, *33*). Moreover, the relative population of each extrahelical guanine in the presence of the octahedral model complex NiHFGN (Figure 7B) remains within 10% of that measured in the absence of any divalent metal ion (*32*).

Direct interaction between NiHFGN and g3/c2 was again characterized best by the shifts in proton resonance caused by Fermi contact to the paramagnetic complex. Although selective line broadening was also observed, the anisotropy of the dipolar effect and the lack of sufficient spectral dispersion (Figure 6) limited its utility. The H8 signals of the three potentially extrahelical guanines, G5, G6, and G7, were originally expected to shift in accord with their relative reactivity (Figure 7A). However, this was not observed (Figure 7C). NiHFGN shifted the signal of G5 H8 to the greatest extent (Figure 6B) even though the extrahelical G5 structure had an abundance of only 26% (Figure 7A,B). The magnitude of this shift is comparable to that of the sole extrahelical guanine in g3/cg4. G6, the most reactive and abundant extrahelical guanine in g3/c2, exhibited an intermediate shift in its H8 resonance, and G7, forming a minor extrahelical species, exhibited approximately no shift in its H8 resonance.

The lack of correlation between the relative reactivity and paramagnetic shifts for g3/c2 is likely a function of the proximity of competing binding sites. In the major groove, perturbations transmit in a 5′ orientation (*22*−*25*). Thus, the observed contact shift of G5 H8 would result from direct NiHFGN coordination to G5 N7 as well as to the N7 groups of G6 and G7. Comparable shifts of G6 H8 would result from only coordination to G6 and G7, and shifts of G7 H8 would result from coordination to G7 alone. This pattern is not limited to the guanine track. The H8 signal of G15, a 5′-neighbor of the guanine track, exhibited a contact shift nearly as large as that of G6 H8 (Figure 6B). Similarly, H8 signals of G5 and G15 exhibited contact shifts upon NiHFGN binding to the lone extrahelical G17 in g3/cg4 (Figure 2B).

CONCLUSION

Selective association between nickel and guanine N7 had long been proposed to control the specificity of nickel reagents used to probe nucleic acid structure (*5*−*7*). In contrast to the action of dimethyl sulfate, target modification by nickel likely requires coordination prior to reaction (*8*). The first direct evidence for such a coordination has now been obtained by the paramagnetic effects of a model nickel complex on an oligonucleotide duplex containing a unique extrahelical guanine. This residue was the primary target of both NiCR oxidation and NiHFGN association. Both nickel-dependent recognition and reaction also appear to proceed without affecting the overall conformation of DNA. Consequently, the reaction profile generated by the reactive nickel complexes should accurately reflect the native equilibrium of nucleic acid structures in solution. Noncanonical guanine residues may now also be characterized by coordination to paramagnetic complexes such as NiHFGN as long as the sites of interest form independent binding domains.

ACKNOWLEDGMENT

We thank Drs. James Muller and Chien-Chung Cheng for their generous gifts of the essential nickel complexes and Drs. Yiu-fai Lam and Jeff Davis for advice and help with the NMR experiments.

SUPPORTING INFORMATION AVAILABLE

Representative NOESY spectra for ^{1}H assignments of g3/cg4 and g3/c2 and tables summarizing assignments and NiHFGN titration of the imino protons of g3/cg4 (6 pages). This material is available free of charge via the Internet at http://pubs.acs.org.

REFERENCES

1. Ehresmann, C., Baudin, F., Mougel, M., Romby, P., Ebel, J.-P., and Ehresmann, B. (1987) *Nucleic Acids Res. 15*, 9109−9129.
2. Nielsen, P. E. (1990) *J. Mol. Recognit. 3*, 1−25.
3. Lilley, D. M. J., and Dahlberg, J. E., Eds. (1992) *Methods Enzymol. 211*, sections III and IV.

4. Tullius, T. D. (1996) in *Bioorganic Chemistry: Nucleic Acids* (Hecht, S. M., Ed.) pp 144−162, Oxford University Press, New York.
5. Burrows, C. J., and Rokita, S. E. (1994) *Acc. Chem. Res. 27*, 295−301.
6. Burrows, C. J., and Rokita, S. E. (1995) *Met. Ions Biol. Syst. 32*, 537−560.
7. Rokita, S. E., and Burrows, C. J. (1999) in *Current Protocols in Nucleic Acid Chemistry* (Glick, G., Ed.) Wiley, New York (in press).
8. Muller, J. G., Zheng, P., Rokita, S. E., and Burrows, C. J. (1996) *J. Am. Chem. Soc. 118*, 2320−2325.
9. Muller, J. G., Hickerson, R. P., Perez, R. J., and Burrows, C. J. (1997) *J. Am. Chem. Soc. 119*, 1501−1506.
10. Chen, X., Woodson, S. A., Burrows, C. J, and Rokita, S. E. (1993) *Biochemistry 32*, 7610−7616.
11. Shih, H.-C., Tang, N., Burrows, C. J., and Rokita, S. E. (1998) *J. Am. Chem. Soc. 120*, 3284−3288.
12. Tang, N., Muller, J. G., Burrows, C. J., and Rokita, S. E. (1999) *Biochemistry* (in press).
13. Butcher, S. E., and Burke, J. M. (1994) *J. Mol. Biol. 244*, 52−63.
14. Chen, X., Chamorro, M., Lee, S. I., Shen, L. X., Hines, J. V., Tinoco, I., and Varmus, H. E. (1995) *EMBO J. 14*, 842−852.
15. Hickerson, R. P., Watkins-Sims, C. D., Burrows, C. J., Atkins, J. F., Gesteland, R. F., and Feldin, B. (1998) *J. Mol. Biol. 279*, 577−587.
16. Pan, J., and Woodson, S. A. (1998) *J. Mol. Biol. 280*, 597−609.
17. Zheng, P., Burrows, C. J., and Rokita, S. E. (1998) *Biochemistry 37*, 2207−2214.
18. Muller, J. G., Chen, X., Dadiz, A. C., Rokita, S. E., and Burrows, C. J. (1992) *J. Am. Chem. Soc. 114*, 6407−6411.
19. Martin, R. B. (1985) *Acc. Chem. Res. 18*, 32−38.
20. Eichhorn, G. L., and Shin, Y. A. (1968) *J. Am. Chem. Soc. 90*, 7323−7328.
21. deMeester, P., Goodgame, D. M. L., Skapski, A. C., and Smith, B. T. (1974) *Biochim. Biophys. Acta 340*, 113−115.
22. Abrescia, N. G. A., Malinina, L., Fernandez, L. G., Huynh-Dinh, T., Neidle, S., and Subirana, J. A. (1999) *Nucleic Acids Res. 27*, 1593−1599.
23. Moldrheim, E., Andersen, B., Frøystein, N., and Sletten, E. (1998) *Inorg. Chim. Acta 273*, 41−46.
24. Gao, Y.-G., Sriram, M., and Wang, A. H.-J. (1993) *Nucleic Acids Res. 21*, 4093−4104.
25. Frøystein, N. A., Davis, J. T., Reid, B. R., and Sletten, E. (1993) *Acta Chem. Scand. 47*, 649−657.
26. Taboury, J. A., Bourtayre, P., Liquier, J., and Taillandier, E. (1984) *Nucleic Acids Res. 12*, 4245−4257.
27. Cheng, C.-C. (1993) Ph.D. Dissertation, State University of New York, Stony Brook, New York.
28. Karn, J. L., and Busch, D. H. (1969) *Inorg. Chem. 8*, 1149−1153.
29. Cheng, C.-C., Rokita, S. E., and Burrows, C. J. (1993) *Angew. Chem., Int. Ed. Engl. 32*, 277−278.
30. Chen, X., Burrows, C. J., and Rokita, S. E. (1992) *J. Am. Chem. Soc. 114*, 322−325.
31. Fasman, G., Ed. (1975) *Handbook of Biochemistry and Molecular Biology−Nucleic Acids*, 3rd ed., Vol. 1, p 589, CRC Press, Boca Raton, FL.
32. Woodson, S. A., and Crothers, D. M. (1988) *Biochemistry 27*, 436−445.
33. Woodson, S. A., and Crothers, D. M. (1988) *Biochemistry 27*, 3130−3141.
34. Scheek, R. M., Boelens, R., Russo, N., van Boom, J. H., and Kaptein, R. (1984) *Biochemistry 23*, 1371−1376.
35. Feigon, J., Sklenar, V., Wang, E., Gilbert, D., Macaya, R. F., and Schultze, P. (1992) *Methods Enzymol. 211*, 235−253.
36. Sletten, E., and Frøystein, N. A. (1996) *Met. Ions Biol. Syst. 32*, 397−418.
37. Woodson, S. (1987) Ph.D. Dissertation, Yale University, New Haven, CT.
38. Sorokin, V. A., Sysa, I. V., Valeev, V. A., Gladchenko, G. O., Degtyar, M. V., and Blagoi, Y. P. (1997) *J. Mol. Struct. 408/409*, 233−236.
39. Jia, X., Zon, G., and Marzilli, L. G. (1991) *Inorg. Chem. 30*, 228−239.
40. Steinkopf, S., Garoufis, A., Nerdal, W., and Sletten, E. (1995) *Acta Chem. Scand. 49*, 495−502.
41. Huang, H., Zhu, L., Reid, B. R., Drobny, G. P., and Hopkins, P. B. (1995) *Science 270*, 1842−1845.
42. Wicholas, M., and Drago, R. S. (1968) *J. Am. Chem. Soc. 90*, 6946−6950.
43. La Mar, G. N., and van Hecke, G. R. (1970) *Inorg. Chem. 9*, 1546−1557.
44. Horrocks, W. D. (1973) in *NMR of Paramagnetic Molecules* (La Mar, G. N., Horrocks, W. D., and Holm, R. H., Eds.) Chapter 4, pp 127−177, Academic Press, New York.
45. Bertini, I., and Luchinat, C. (1986) *NMR of Paramagnetic Molecules in Biological Systems*, Benjamin/Cummings, Reading, MA.
46. Rehmann, J. P., and Barton, J. K. (1990) *Biochemistry 29*, 1710−1717.
47. Kagawa, T. F., Geierstanger, B. H., Wang, A. H.-J., and Ho, P. S. (1991) *J. Biol. Chem. 266*, 20175−20184.
48. Maxam, A. M., and Gilbert, W. (1980) *Methods Enzymol. 65*, 499−560.

BI991877H